Bashivan, P., Bidelman, G. M., &Yeasin, M. (2013). Neural correlates of visual working memory load through unsupervised spatial filtering of EEG. Proceedings of Machine Learning and Interpretation in Neuroimaging (MLINI'13), Lake Tahoe, NV, December 9–10, 2013.

Neural correlates of visual working memory load through unsupervised spatial filtering of EEG

Pouya Bashivan[1] , Gavin M. Bidelman[2], Mohammed Yeasin[1,*]

[1] Computer Vision, Perception, and Image Analysis Lab, [2]Auditory Cognitive Neuroscience Lab, University of Memphis, Memphis, TN, United States
{pbshivan, gmbdlman, myeasin}@memphis.edu

Abstract. Understanding the neural basis of working memory (WM) is critical to study of the higher level cognitive processes. The WM load and the confluence of related features can be used to characterize many cognitive processes and their limits. In particular, to study the neural correlates of visual working memory load, we recorded multichannel EEG during a visual WM task which varied in difficulty. A set of features extracted from the event-related potentials (ERPs) and event-related synchronization/desynchronization (ERS/ERD) were used to quantify changes in activation with increasing WM demands. To further our understanding of relationship between the stimuli and the underlying neural processes, Independent component analysis (ICA) was used on EEG data for spatial filtering. Common independent components across variation in task difficulties were then found by clustering the ICs and used to investigate changes in brain activity with increasing memory load. It was observed that temporal properties of ERPs obtained from the independent components are highly distinguishable as opposed to traditional region of interest (ROI) approach. This result suggests that more representative neural correlates could be obtained by using this technique.

Keywords: EEG, time-frequency analysis, event-related synchronization, independent component analysis, working memory capacity, cognitive load

1 Introduction

Working memory (WM) is considered a limited resource shared among a number of different higher-level cognitive functions (e.g., language, planning, problem-solving). WM is a storage to maintain and manipulate the information during more complex mental functions [1]. Event-related potentials (ERP) and event-related desynchronization/synchronization (ERD/ERS) [2] are two well-established methods that can be used to understand cognitive processes via patterns of scalp-recorded brain activity [3]. Different waves of the temporal ERP signal including N100, P300, and late positive wave (LPW) have been shown to correlate with memory load [4], [5], [6]. Likewise, studies have shown that spectral measures (i.e., ERD/ERS) within different frequency bands show strong correspondence with WM load [7], [8].

In previous studies, neural correlates of WM have been investigated by comparing responses recorded at single electrode sites from localized regions of the brain [4], [7]. Although, previous studies have revealed the existence of spectro-temporal perturbations related to memory operation but very little effort has been made to apply

these correlates toward understanding their dynamics with changing memory load. Independent component analysis (ICA) is an unsupervised spatial filtering method which can also be used to separate different rhythmic EEG components, such as right- and left-hemispheric mu rhythms from EEG [9]. Here, we investigated changes in those ICs which were shared among different levels of difficulty during a WM task to understand the common sources of neural activity engaged by this cognitive process and how (also which of) these networks are modulated by task demands. Task difficulty was parametrically manipulated by varying the amount of memory effort required to complete a visual WM task. It was predicted that neural activity (as measured by spectro-temporal features of the EEG) would vary monotonically with increasing memory load and that neural responses would saturate beyond an individual's memory capacity limit (as measured behaviorally).

2 Materials & Methods

2.1 Subjects

Ten healthy, right-handed [10] individuals (5 males, 5 females) participated in this study. Participants were between 24 and 33 years of age (M = 29.3, SD = 3). None reported any neurological disorders or were on medication. All participants gave informed consent according to procedures approved by University of Memphis institutional review board and were compensated for their time.

2.2 Visual WM task and stimuli

We adopted a modified version of the well-established Sternberg memory task [11]. On each trial, subjects briefly (500ms) observed a matrix consisting of different English characters positioned around a center point ("SET"; Fig. 1). The size of each character was 1.8°; they were distributed around a center fixation cross and within a visual angle of 4.5°. Array size varied randomly (2, 4, 6 or 8 items). After a 3s delay, a "TEST" character was shown in the center of the screen. Subjects responded via a button press to indicate if this character had occurred in the previous memory "SET". On half the trials, the test item occurred in the set; the other half it did not. Subjects were encouraged to respond as accurately as possible and feedback was given via a colored light on the screen. The next trial was initiated after a 3.4 sec inter-stimulus interval. Following 20 practice trials for task familiarization, subjects completed 60 experimental trials per set-size condition.

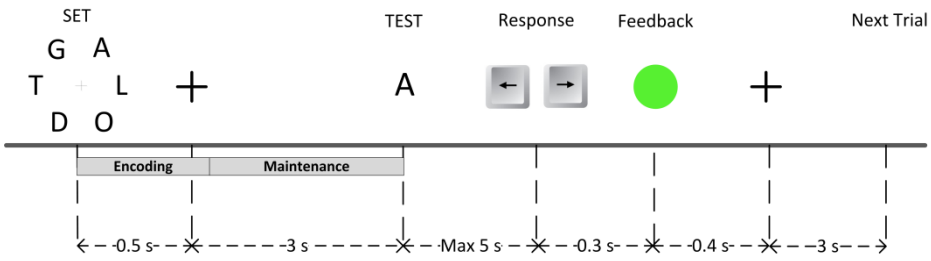

Fig. 1. Time-course of the WM stimulus paradigm

Subjects were seated inside an electro-acoustically shielded booth. They were instructed to avoid body movement and restrict their visual gaze during the task by fixating on the center of the screen. The visual WM task was presented on a LCD monitor at a distance of 1 m. Length of single block of experiment was 14.4 min plus response time. A 5 min break time was given between conditions blocks.

2.3 EEG Recording

The continuous EEG was recorded from 64 sintered Ag/AgCl electrodes around the scalp at standard 10-20 locations (Neuroscan-Quik-cap). Electrodes placed on the outer canthi of the eyes and the superior and inferior orbit were used to monitor ocular activity. Data were digitized with a sampling rate of 500Hz and a filter passband from DC-250 Hz. Electrode impedance was maintained $\leq$5kΩ over the course of the experiment. Neuroelectric data are presented with a common average reference (CAR).

2.4 EEG Preprocessing and analysis

EEG data were down-sampled to 250Hz, and base-line corrected by removing the average of each channel. Ocular artifacts (saccades and blink artifacts) were corrected in the EEG using a principal component analysis (PCA) [12]. Responses were then band-pass filtered from 1 to 45Hz for visualization and response quantification.

ERP signals were computed by averaging over all trials with correct responses and baseline corrected in reference to a 200ms window prior to stimulus presentation. Likewise, event-related spectral perturbation (ERSP) responses were generated using the same set of trials and a 2-sec window prior to stimulus presentation as the reference period. Procedures to compute ERP, ERS/ERD and ERSP are thoroughly explained in [13], [2], [3].

2.5 Component Clustering

In order to improve the clarity of activity signals, we performed ICA on the epoched EEG data. To avoid any pre-assumptions on how brain responds when the memory is overloaded or not, we considered each condition of the experiment as independent tasks. Trials corresponding to each memory set size were bundled together in separate datasets. ICA algorithm was performed yielding 64 independent components (ICs) per dataset. We chose the maximum number of extractable components (64) to segregate independent activity signals with the highest precision available to us. Projection vectors corresponding to each IC were then extracted from the mixing matrix (W^{-1}). Another dataset consisting of all projection vectors were formed (256 vectors from 4 datasets) and a clustering method was run on the dataset to find distinct clusters. We assumed that each of the 64 ICs represents a separate class of activity with roughly distinct projection vector. Moreover, the number of ICs which could be shared across the four tasks will be maximally equal to 64. We used the k-means clustering [14] to find the ICs with similar projection patterns. The number of separate clusters was chosen as 64, equal to number of ICs for each task.

By running the k-means algorithm on the dataset of projection weight vectors, we intended to cluster those activity signals that were projected to the electrodes with the same pattern across the various memory loads. We are only interested in those clus-

ters which represent common source activity modulated by WM demands. Thus, we focused on the common components appearing in all four set size conditions. As such, 28 component clusters were found which contained components from all four conditions. Fig. 2 shows the projection map of 10 of these components, which showed significant changes across set-sizes, with the cluster's centroid as the projection vector.

Frequency bands for each subject were tuned in reference to their individual α-frequency (IAF) [15]. IAF was considered as the frequency with maximum power within the α-band. The IAF was determined by analyzing a 2 min resting EEG recording for each subject with eyes closed. θ-, α-, and β-frequency bands were then defined as [IAF-4 Hz to IAF-2 Hz], [IAF-2 Hz to IAF+2 Hz] and [IAF+2 Hz to 30 Hz], respectively. Electrodes were grouped into 10 regions of interest (ROI) around the scalp (Fig. 3).

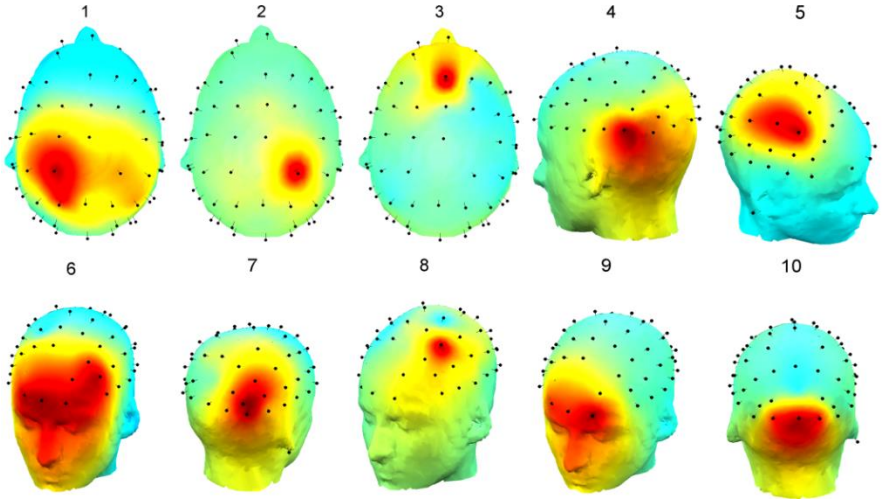

Fig. 2. Scalp maps of 10 common independent components with increasing WM load. Warmer colors correspond to higher weights.

In order to investigate whether WM load modulated responses over the encoding or maintenance period (Fig. 1), different features were defined from the EEG signal over the time course of the task:

1. **ERP magnitude:** The difference between maximum positivity and negativity in the ERP signal, occurring from 50-700 ms after presentation of the stimulus array (Fig. 4).
2. **Total θ ERD encoding**: the sum of alpha ERD measured during the period in which the ERD signal was greater than ¼ of the maximum ERD.
3. **Total α ERD:** the sum of alpha ERD measure over the encoding and maintenance period.

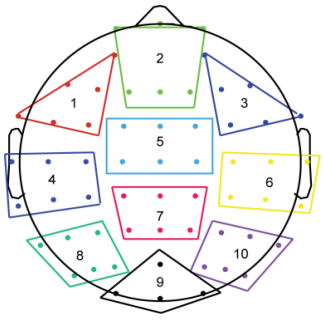

Fig. 3. Division of electrodes into ROIs.

4. **Total β ERD of encoding**: the sum of beta ERD measure during the period in which the ERD signal was greater than ¼ of the maximum ERD.
5. **Total β ERD**: the sum of beta ERD measure over the encoding and maintenance period.
6. **Total θ ERD:** the sum of theta ERD measure over the encoding and maintenance period.

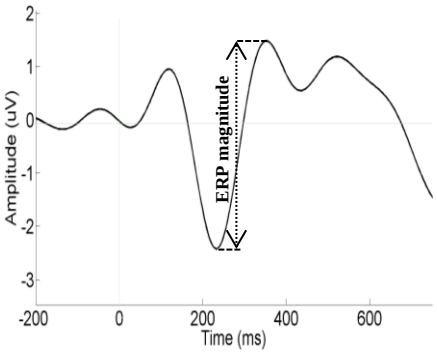

Fig. 4. ERP magnitude. *t*=0 represents the onset of presentation of the stimulus "SET".

3 Results

Participants performed well in small set size conditions (2, 4 items); performance degraded precipitously with increasing set size (> 6 items). Mean (SD) response accuracy were 94.5 (4.4)%, 93.6 (4.4)%, 79.2(6.1)% and 66.8 (7.04)% for set sizes 2, 4, 6 and 8, respectively.

Within each EEG cluster, if multiple components from single condition existed, the component with the highest mean projected variance was selected. We used repeated measures ANOVA to quantify the variability of the measurements across conditions and subjects. Table-1 illustrates the components as well as electrode regions which showed significant (p<0.05) variation in the response feature across stimulus set sizes. Results from the ROI approach which has repeatedly been used in the study of memory load [4, 7, 8] were also included for comparison purposes.

Table 1. Electrode ROIs /ICs with significant changes across stimulus conditions.

Feature type	ROI number	IC number
ERP magnitude	5^{*}	2^{*}, 4^{***}, $5^{¤}$, 6^{*}, 8^{**}, $9^{¤}$
Total Encod. α ERD	1^{*}, 5^{*}, $7^{¤}$, 9^{*}, 10^{**}	1^{*}, 5^{*}, 7^{**}, 8^{*}, 10^{**}
Total α ERD	5^{*}, 7^{***}, 9^{*}, 10^{*}	1^{*}, 3^{*}, 5^{**}, 7^{*}, 10^{**}
Total Encod. β ERD	7^{*}	1^{*}, 7^{*}, 10^{*}
Total β ERD	-	3^{*}, 10^{*}
Total θ ERD	5^{**}, 7^{**}	1^{*}, 3^{*}, 8^{*}, 10^{*}

*p<0.05, **p<0.01, ***p<0.001, ¤p<0.0001

It is clear from Table-1 that the features extracted from the ICs are far more distinctive than those obtained from the ROI approach, especially for the ERP magnitude feature. As an example, ERSP of the component cluster 1 is illustrated in Fig. 5. This figure shows a build-up of the response during the encoding period which extends with increasing memory load. The main activity in this component which exists in all three frequency bands (more dominant in α-band) beginning ~200ms after presentation of the "SET" array and extending up to 2400ms after the cessation of stimulus presentation.

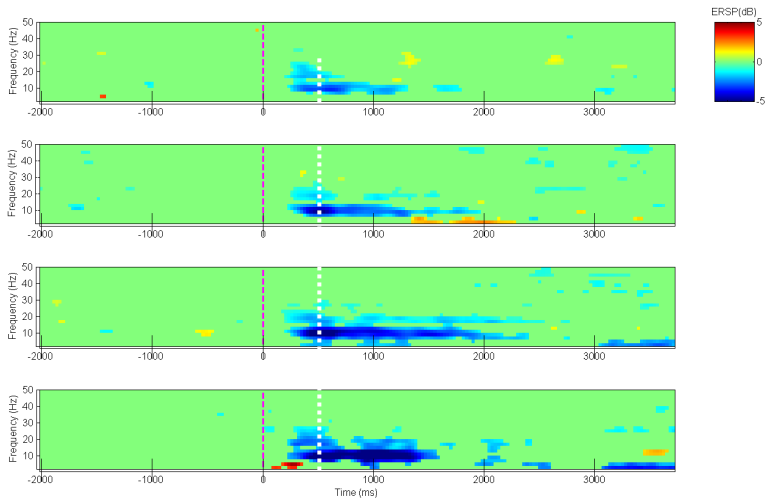

Fig. 5. ERSP comparison across conditions for component cluster 1 during the encoding and maintenance periods. Rows 1-4 illustrate the response to stimulus set-sizes 2, 4, 6 and 8 respectively. The dotted line demarcates the cessation of the stimulus "SET" presentation.

4 Discussion

In this study, we examined the effect of memory load by comparing changes in spectro-temporal features of evoked brain activity during a visual WM task. The ERPs showed that neural activity in fronto-central areas covaried well with stimulus array set size and hence, task difficulty. Changes in the ERD α-power across conditions were also observed during the encoding period of the visual stimuli particularly in postero-central locations. More posterior electrode locations also showed significant changes in β- and θ -power during the encoding and maintenance period.

In comparison, ICs of evoked brain activity revealed significant WM load-induced changes originated from source components 1, 3, 5, 7, 8 and 10 which spanned both fronto-central and postero-central networks (Fig. 2). Component time courses not only explain the recordings in each area but also provide a means to understand how their source networks are distributed spatially. Furthermore, this method also revealed task-relevant activity (e.g., θ-band ERD) in frontal regions otherwise unobservable in the conventional ERP averages. The trend of changes in almost all spectral features and all positions/components with high significance showed a steady increase between set-sizes 2, 4 and 6 but a decrease from 6 to 8. This non-monotonic nature of neural responses and parallel pattern in behavioral accuracy implies that subjects reached a cognitive overload after a set size ~6 items. Our electrophysiological results are also consistent with previous findings from EEG and fMRI studies [16], [7], [17]. While compared to traditional ROI analysis, the IC study delivers a much more accurate spatial estimation (as compared to the ROI approach which divides the cortex area into a predefined number of regions) that preserves the spectro-temporal characteristics of the activities. In addition, IC comparisons showed significant changes in β- and θ- bands in frontal and occipital regions unobservable in electrode ROIs measures.

5 Conclusions

Spatial filtering is an effective method for extraction of features with higher sensitivity and robustness. In the current study, spatial filtering was used to separate different components during each variation of the same task and the common components across the variations were then sought using an unsupervised clustering method. It was observed that ICA based spatial filtering offers a means to distinguish neurophysiological activity underlying cognitive processing with higher sensitivity than traditional EEG methodology. This work is an important step towards our future work in modeling the memory load from EEG signals.

References

1. A.D. Baddeley, Working memory. New york: Oxford Univ. Press, 1986.
2. G. Pfurtscheller and F.H. Lopes da Silva, "Event-related EEG/MEG synchronization and desynchronization: basic principles," Clinical Neurophysiology, vol. 110, pp. 1842-1857, 1999.
3. Donald L. Schomer and Fernando Lopes da silva, Niedermeyer's electroencephalography: Basic principles, clinical applications, and related fields.: Wolters Kluwer Health, 2012.
4. Edward K. Vogel and Maro G. Machizawa, "Neural activity predicts individual differences in visual working memory capacity," Nature, pp. 748-750, 2004.
5. Edward J. Golob and Arnold Starr, "Serial position effects in auditory event-related potentials during working memory retrieval," Journal of Cognitive Neuroscience, pp. 40-52, 2004.
6. Shiho Okuhata, Takuya Kusanagi, Hirokazu Kawaguchi, and Tetsuo Kobayashi, "Sequential memory scanning during Sterberg memory task regardless of the different presentation style," in Internationl Conference on Complex Medical Engineering, Kobe, Japan, 2012, pp. 86-89.
7. Christina M. Krause, Lauri Sillanmaki, Mika Koivisto, and Carina Saarela, "The effects of memory load on event-related EEG desynchronization and synchronization," Clinical Neurophysiology, pp. 2071-2078, 2000.
8. A. Stipacek, R. H. Grabner, C. Neuper, A. Fink, and A.C. Neubauer, "Sensitivity of human EEG alpha band desynchronization to different working memory components and increasing levels of memory load," Neuroscience Letters, pp. 193-196, 2003.
9. S. Makeig, S. Debener, J. Onton, and A. Delorme, "Mining event-related brain dynamics," Trends Cogn. Sci., vol. 8, pp. 204-210, 2004.
10. R.C. Oldfield, "The assessment and analysis of handedness: the Edinburgh inventory.," Neuropsychologia, vol. 9, pp. 97-113, 1971.
11. S. Sternberg, "High-speed scanning in human memory," Science, vol. 153, pp. 652-654, August 1966.
12. G.L. Wallstrom, R.E. Kass, A. Miller, J.F. Cohn, and N.A. Fox, "Automatic correction of ocular artifacts in the EEG: a comparison of regression-based and component-based methods.," Int. J. Psychophysiol., vol. 53, pp. 105-119, 2004.
13. S.J Luck, An introduction to the event-related potential technique., 2005.
14. R. Duda, P.E. Hart, and D.G. Stork, Pattern classification.: John Wiley & Sons, 2012.
15. W. Klimesch, "EEG alpha and theta oscillations reflect cognitive and memory performance: a review and analysis," Brain Res., vol. 29, pp. 169-195, 1999.
16. Jonathan D. Cohen et al., "Temporal dyncamics of brain activation during a working memory task," Nature, vol. 386, pp. 604-607, April 1997.

17. Matthew P. Kirschen, S. H. Annabel Chen, and John E. Desmond, "Modality specific cerebro-cerebellar activations in verbal working memory: an fMRI study," Behav. Neurol., vol. 23, pp. 51-63, 2010.
18. Christina M. Krause, A. Heikki Lang, Matti Laine, Mika Kuusisto, and Bodil Porn, "Event-related EEG desynchronization and synchronization during an auditory memory task," Electroencephalography and clinical Neurophysiology, vol. 98, pp. 319-326, 1996.